# Magnetic orders and topological phases from $f$-$d$ exchange in pyrochlore iridates

Gang Chen and Michael Hermele
*Physics Department, University of Colorado, Boulder, Colorado 80309, USA*
(Received 1 September 2012; published 19 December 2012)

We study theoretically the effects of $f$-$d$ magnetic exchange interaction in the $R_2Ir_2O_7$ pyrochlore iridates. The $R^{3+}$ $f$ electrons form localized Kramers or non-Kramers doublets, while the $Ir^{4+}$ $d$ electrons are more itinerant and feel a strong spin-orbit coupling. We construct and analyze a minimal model capturing this physics, treating the Ir subsystem using a Hubbard-type model. First neglecting the Hubbard interaction, we find Weyl semimetal and Axion insulator phases induced by the $f$-$d$ exchange. Next, we find that $f$-$d$ exchange can cooperate with the Hubbard interaction to stabilize the Weyl semimetal over a larger region of parameter space than when it is induced by $d$-electron correlations alone. Applications to experiments are discussed.

DOI: 10.1103/PhysRevB.86.235129 PACS number(s): 71.27.+a, 71.70.Ej

The discovery of time-reversal invariant topological band insulators has opened new terrain in the study of topological states of matter.[1–3] As spin-orbit coupling (SOC) is essential to realize some topological states, and given the propensity of electron correlations to induce a variety of novel phenomena, there is now intense interest in 5$d$ transition metal oxides with simultaneously strong SOC and intermediate electron correlation. The pyrochlore iridates $R_2Ir_2O_7$, where R is a lanthanide (or Y), have been proposed to host various topological phases. Topological band insulators, topological Mott insulators[4], and Weyl semimetal (WSM) states[5] have been proposed.[4–7] In the related spinel compounds $A_2Os_4O_6$, an Axion insulator (AI)[5,8–11] with bulk magnetic order and large magnetoelectric effect has been proposed.[12]

The current theoretical analyses of pyrochlore iridates have focused *either* on the Ir subsystem,[4–7,13] *or* (excluding nonmagnetic R = Y, Eu) on the magnetic moments formed by localized $R^{3+}$ $f$ electrons.[14–18] However, as we argue below, coupling between the local moments and the $Ir^{4+}$ $d$ electrons may be important in some compounds, but remains largely unexplored (see Refs. 19–21 for related prior work). More generally, most work on correlated, strong SOC materials is focused on correlations among $d$ electrons. An alternate route to introduce correlation into a strong SOC system is to couple strong-SOC itinerant carriers to local magnetic moments, and such systems are certainly deserving of greater attention.

In this paper we consider the effect of $f$-$d$ exchange in pyrochlore iridates. The $f$-$d$ exchange and the Ir electrons together generate a RKKY exchange between the localized moments at the R sites, which induces magnetic ordering on the R subsystem. The magnetic order on the R subsystem further modifies the electronic structure on the Ir subsystem, leading to WSM and Axion insulator phases. Notably, when $f$-$d$ exchange is combined with correlation of the $d$ electrons, we find the WSM is stabilized over a much wider region of parameter space than was found for $d$-electron correlations alone.[6] Based in part on this observation, we propose that $Nd_2Ir_2O_7$ is a candidate to realize the WSM.

In many pyrochlore iridates, a metal-insulator transition and/or magnetic order occurs at a temperature scale of $\sim$100 K. Such a scale is presumably too large to be driven by RKKY interaction, and instead is probably set by $d$-electron magnetic exchange interaction, so the emphasis on the Ir subsystem may be justified. However, in some compounds, interesting transport and magnetic properties only occur at lower temperatures. For instance, in $Pr_2Ir_2O_7$, a chiral spin liquid phase has been proposed at $0.3 < T < 1.5$ K to account for the anomalous hall effect observed in this temperature window, where no clear signature of magnetic order is observed.[22] In $Nd_2Ir_2O_7$, the metal-insulator transition, which seems to be associated with magnetic order, occurs at 36 K and can be suppressed by the application of pressure.[23–25] It should be noted that other studies of the Nd compound show different behavior, apparently due to differences in sample preparation.[26,27]

We now describe our theoretical model for $R_2Ir_2O_7$. The R and Ir sites each form a pyrochlore lattice of corner-sharing tetrahedra. The non-Kramers $R^{3+}$ ions (R = Pr, Tb, Ho) have an even number of $f$ electrons, while the Kramers ions (R = Nd, Sm, Gd, Dy, Yb) have an odd number of $f$ electrons. The large SOC of $f$ electrons then leads to a local magnetic moment with integer (non-Kramers) or half-odd-integer (Kramers) total angular momentum $J$. The $(2J+1)$-fold degeneracy is then split by the $D_{3d}$ crystal field at the R site. In the Kramers case, this leads to a doublet ground state. In the non-Kramers case, the crystal field splits the angular momentum multiplet into doublets and nonmagnetic singlets. A non-Kramers doublet is the ground state for the R = Pr iridate,[15,16] as well as for isostructural insulating compounds like $Tb_2Ti_2O_7$ and $Ho_2Ti_2O_7$,[28,29] so we assume a doublet ground state. We ignore effects of higher crystal field levels, which is valid for sufficiently large energy gap between the crystal field ground state and first excited state. This is reasonable for the R = Pr, Nd cases of greatest interest, where the reported gaps are 168 and 300 K, respectively.[30,31] The R-site moment is thus described in all cases by an effective spin-1/2 pseudospin $\boldsymbol{\tau}$. The $d$ electrons of the Ir subsystem are more itinerant. Due to the strong SOC, we approximate the Ir subsystem as a pyrochlore lattice system with one $j_{\text{eff}} = 1/2$ doublet electron per Ir site.[6]

For the exchange coupling between R pseudospin $\boldsymbol{\tau}$ and Ir effective spin $\mathbf{j}$, we invoke a general symmetry analysis, beginning with the non-Kramers case. Under time reversal, $\tau^z \to -\tau^z, \tau^{x,y} \to \tau^{x,y}$. [This is so because $\tau^z$ originates from $J^z$, the component of angular momentum along the local threefold axis at the R site, while $\tau^{x,y}$ originate from $(J^{\pm})^{2J}$, where $J$ is the total angular momentum.] On the

 

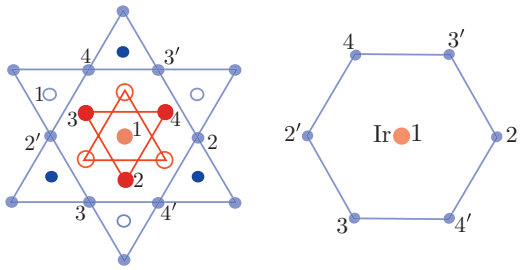


FIG. 1. (Color online) A projective view of $R_2Ir_2O_7$ in the (111) plane. Left: The neighboring Ir (in dark red) and R (in light blue) tetrahedra. "1,2,3,4" label the four sublattices. Ir/R atoms are marked with big/small (red/blue) circles. Empty/dark/light circles indicate that the atoms are below/above/in the (111) plane. Right: An $IrR_6$ complex singled out from the left figure.

other hand, under time reversal $\mathbf{j} \to -\mathbf{j}$. This property leads to a remarkable simplification of the coupling—only $\tau^z$ couples to the Ir spin $\mathbf{j}$. We consider the nearest-neighbor (NN) R-Ir exchange, which, due to space group symmetry, is parametrized by two couplings $c_1,c_2$. For the single Ir site labeled Ir1 in Fig. 1, the $f$-$d$ exchange is

$$\mathcal{H}_{\rm fd} = \left[c_1\tau_4^z - c_2\left(\tau_2^z+\tau_3^z\right)\right]j_1^x + \left[c_1\tau_3^z - c_2\left(\tau_2^z+\tau_4^z\right)\right]j_1^y + \left[c_1\tau_2^z - c_2\left(\tau_3^z+\tau_4^z\right)\right]j_1^z + [2\leftrightarrow 2',3\leftrightarrow 3',4\leftrightarrow 4'], \tag{1}$$

where the labeling of sites is given in Fig. 1. Further details are given in Appendix. A.

In the Kramers case, the Ising part of the $f$-$d$ exchange (coupling of $\tau^z$ to $\mathbf{j}$) is identical. Transverse exchange involving $\tau^{x,y}$ is also permitted by time-reversal symmetry. Even in the non-Kramers case, while $\tau^{x,y}$ does not couple to the Ir effective spin, it can couple to the Ir charge density. In both cases we ignore these transverse couplings, both for simplicity and because they may be suppressed by strong easy-axis anisotropy of the $f$ moments along local [111] axes, which is known to be present in R = Dy, Ho pyrochlore oxides,[14] and may be present more broadly. However, effects of transverse exchange may be important, and will be an interesting topic for future study.

For the Ir subsystem, we follow Ref. 6 and include both the indirect hopping of $5d$ electrons through oxygen, and direct hopping between Ir sites, using the following Hubbard model:

$$\mathcal{H}_{\rm Ir} = \sum_{\langle rr'\rangle}\left(\mathcal{T}^d_{rr',\alpha\beta} + \mathcal{T}^{\rm id}_{rr',\alpha\beta}\right)d^\dagger_{r\alpha}d_{r'\beta} + U\sum_r n_{r,\uparrow}n_{r,\downarrow}, \tag{2}$$

where $d^\dagger_{r,\alpha}$ is the electron creation operator, with $\alpha = \uparrow, \downarrow$ labeling the effective spin $j^z = 1/2, -1/2$ states at site $r$, and $n_{r,\alpha} = d^\dagger_{r,\alpha}d_{r,\alpha}$. The sum is over NN pairs of Ir sites. The direct hoppings ($\mathcal{T}^d_{rr'}$) involve two parameters,[6] $t_\sigma$ and $t_\pi$, that describe the $\sigma$ and $\pi$ bonding, respectively. To be specific, we follow Ref. 6 and set $t_\pi = -\frac{2}{3}t_\sigma$ throughout the paper. The indirect hopping ($\mathcal{T}^{\rm id}_{rr'}$) only has one hopping parameter which we denote as $t$.[4]

The R local moments can couple to each other either via superexchange through intermediate atoms, by dipole-dipole interaction, or by the RKKY (Ruderman-Kittel-Kasuya-Yosida) exchange mediated by Ir electrons. Dipole-dipole interactions may play an important role for R (= Gd, Tb, Dy, Ho) where a large local magnetic moment is observed.[26] RKKY exchange is likely to be the dominant exchange for the other compounds, as the Curie-Weiss temperatures in many of the isostructural insulating materials $R_2Sn_2O_7$[32] are of much lower magnitude than the corresponding iridates. For example, The Curie-Weiss temperatures $\Theta_{\rm CW}$ are $-0.35$ K in $Pr_2Sn_2O_7$ and $-10$[26] or $-20$ K[33] in $Pr_2Ir_2O_7$. For the R = Nd compounds, $\Theta_{\rm CW} \approx -0.31$ K in the stannate[32] and $\Theta_{\rm CW} \approx -19$ K in the iridate.[26]

From the above analysis, we obtain our minimal model for $R_2Ir_2O_7$, which includes the R-Ir exchange coupling in Eq. (1) and the Ir-Ir hopping and interaction Eq. (2), $\mathcal{H}_{\rm min} = \mathcal{H}_{\rm fd} + \mathcal{H}_{\rm Ir}$.

To analyze the phase diagram we start with the tight-binding model of the Ir subsystem. Following Ref. 6, a semimetal phase is obtained for $-1.67t \lesssim t_\sigma \lesssim -0.67t$. Otherwise, a strong topological band insulator (STI) with topological class (1;000) is obtained.[34–36] In the semimetal phase, at the $\Gamma$ point there is a quadratic band touching (protected by cubic symmetry) at the Fermi energy ($E_F$). There are also nondispersing bands at $E_F$ along the $\Gamma$-$L$ lines; this feature is a consequence of fine tuning; it can be removed by adding a weak next-nearest-neighbor hopping ($t'$).[6] The low-energy features of the band structure agree rather well with the first-principles calculation for $Y_2Ir_2O_7$,[5,37] with the differences that the quadratic $\Gamma$-point touching is below $E_F$ and the $\Gamma$-$L$ lines have a small dispersion.

Due to the Ising form of the coupling, the model with the $f$-$d$ exchange does not contain quantum fluctuations of the $f$ moments, and reduces to a free fermion problem for any fixed configuration of localized moments. Finding the ground state amounts to finding the minimum-energy configuration of local moments. Moreover, certainly $c_1,c_2 \ll t$, so the $f$-$d$ exchange can be treated perturbatively, and the leading effect is to generate a RKKY exchange between the $f$ moments. As shown in Appendix A, we find that beyond fourth neighbors the RKKY exchange becomes significantly smaller, so we keep only up through fourth-neighbor exchange. Using the Luttinger-Tizsa method,[38] we find that the ground state of the truncated RKKY exchange has a $\mathbf{q} = \mathbf{0}$ magnetic order except in the light shaded regions of Figs. 2(a) and 2(b). In the light shaded regions, the hard-spin constraint cannot be satisfied, and the nature of the ground state is not presently clear. However, it is likely that the $\mathbf{q} = \mathbf{0}$ magnetic order extends at least somewhat into to the light shaded regions.

Without losing any generality, we can simply focus on the case with $c_1 > 0$ and define $\Phi \equiv \tan^{-1}(c_2/c_1)$ and $c \equiv \sqrt{c_1^2 + c_2^2}$. As shown in Figs. 2(a) and 2(b), for most of parameter space, "all-in all-out" magnetic order is favored, where every tetrahedron of neighboring R sites has either all $\tau^z$ pointing in (i.e., toward the tetrahedron center), or all pointing out. In the dark shaded region, $\mathbf{q} = 0$ "two-in two-out" magnetic order is obtained, where on every tetrahedron, two $\tau^z$ point in and two point out. (The $\mathbf{q} = 0$ two-in two-out state also has lowest energy, at least among $\mathbf{q} = 0$ states, in the vertically hatched regions.) Since no ferromagnetic state is observed in any $R_2Ir_2O_7$, we restrict our discussion to all-in all-out state. Such order of the R subsystem also induces all-in all-out

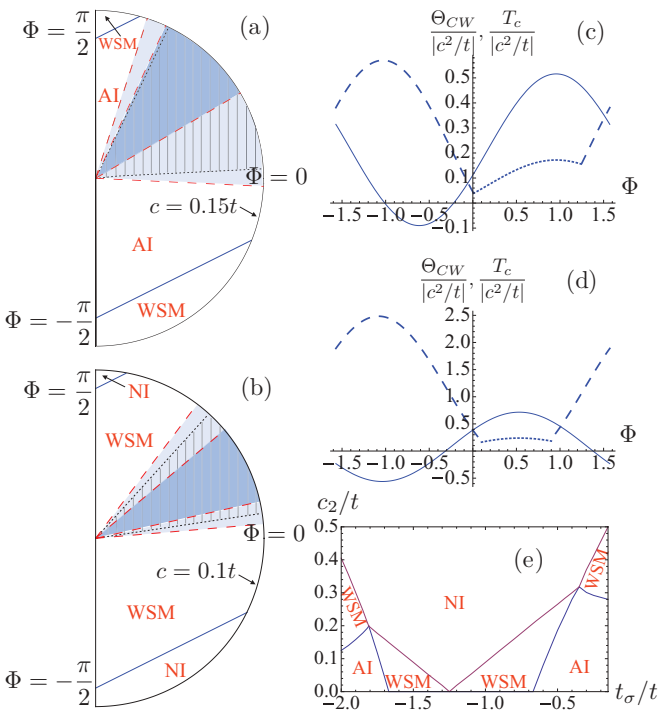


FIG. 2. (Color online) (a) Phase diagrams of the STI with $t_\sigma = -2t$ and (b) the semimetal phase with $t_\sigma = -t$ after including $f$-$d$ exchange. See text for further discussion of the phase diagrams. (c) and (d) Curie-Weiss temperature $\Theta_{\rm CW}$ (solid line) and the mean-field ordering temperature $T_c$ (dashed/dotted line) of the truncated exchange model (up to fourth neighbor for R system) are plotted against $\Phi$. $T_c$ is obtained by restricting to the $\mathbf{q} = \mathbf{0}$ magnetic ordering (see Appendix B). $T_c$ for the all-in all-out (two-in two-out) state is the dashed (dotted) curve. (e) The $c_2$-$t_\sigma$ phase diagram for Ir subsystem where the magnetic order is all-in all-out. In the figure, NI = normal insulator.

magnetic order in the Ir subsystem via the $f$-$d$ exchange, which acts as a local magnetic field modifying the Ir band structure.

As shown in Figs. 2(a) and 2(b), with an $f$-$d$ exchange, the STI phase is converted into an AI for small $c/t$ and then into a WSM. The semimetal phase immediately becomes a WSM. In this case, it is necessary to add a very small $t'$ to stabilize the WSM[6]; otherwise, the flat $\Gamma$-$L$ lines of the semimetal remain at $E_F$.

Returning to the STI case, when time-reversal symmetry is broken but inversion symmetry is preserved, as for the all-in all-out state, the magnetoelectric response parameter $\theta$ is still quantized. We can express $\theta$ in terms of the number $n_o(\mathbf{k})$ of filled odd parity states at the time-reversal invariant momenta (TRIMs),[10,11] $\frac{\theta}{\pi} \equiv \frac{1}{2}\sum_{\mathbf{k}\in\text{TRIMs}} n_o(\mathbf{k})$ (mod 2).

As shown in Fig. 2(a), a region of AI phase with $\theta = \pi$ is obtained in the vicinity of the STI phase and the band structure of an AI induced by $f$-$d$ exchange is shown in Fig. 3(a).

The Fermi surface of WSM is composed of the Weyl points, around which the spectrum is linear and gapless. We locate the Weyl points explicitly by examining the spectrum and density of states, which shows the characteristic $(E - E_F)^2$ scaling. As $c$ increases, the eight Weyl points of the WSM in Fig. 2(b)

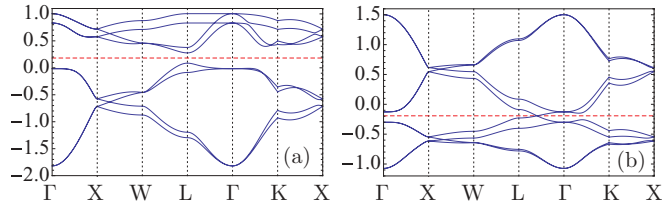


FIG. 3. (Color online) The Ir electron band structure with the all-in all-out magnetic order. The energy unit is set to $t$ and $c_1 = 0, c_2 = 0.05t$. The dashed (red) line is $E_F$. (a) AI phase with $t_\sigma = -2t$. (b) WSM phase with $t_\sigma = -t$.[39]

are created at $\Gamma$ and annihilated at the $L$ points, and lie along the $\Gamma$-$L$ lines [Fig. 3(b)].

We now include the correlation on the Ir subsystem. Without the $f$-$d$ exchange, the Hartree mean-field analysis of the extended Hubbard model on Ir subsystem gives a rather narrow region of WSM phase.[6] With $f$-$d$ exchange, the RKKY exchange induces magnetic order even with weak correlations and thus gives a WSM phase. We start from the metallic phase and include both the Hubbard interaction (via the same mean-field approach used in Ref. 6) and $f$-$d$ exchange. Since both correlation and RKKY interaction alone give an all-in all-out magnetic order on the Ir system, we restrict attention to the all-in all-out state. We decouple the Hubbard interaction,

$$U n_{i\uparrow} n_{i\downarrow} \to -\frac{2U}{3}\mathbf{j}_i^2 \to -\frac{4U}{3}\langle \mathbf{j}_i\rangle \cdot \mathbf{j}_i + \frac{2U}{3}\langle \mathbf{j}_i\rangle^2, \qquad (3)$$

and find a broad region of WSM phase (see Fig. 4).

A much-studied compound in the $R_2Ir_2O_7$ series is R = Pr, which exhibits a metallic ground state and anomalous Hall effect without any observable magnetic order for $0.3 < T < 1.5$ K.[22,33,40] The Pr moments freeze at $T < 0.3$ K. Our theoretical analysis focuses on the all-in all-out region of the phase diagrams in Fig. 2. $Pr_2Ir_2O_7$ may be located in or near the light shaded region of Fig. 2(b), where the RKKY exchange may be more frustrated. Moreover, quantum fluctuations may be important for $Pr_2Ir_2O_7$, perhaps originating from the transverse part of the $f$-$d$ exchange, from superexchange between the $f$ moments,[15] or both. Such quantum fluctuations may suppress the magnetic order, perhaps cooperating with classical frustration.

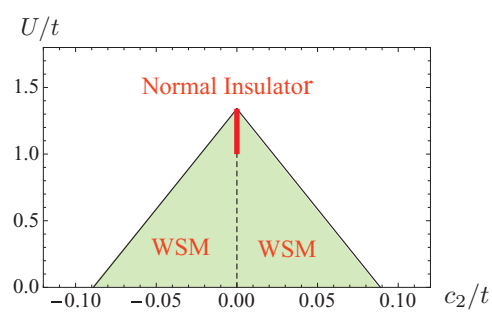


FIG. 4. (Color online) The mean-field phase diagram at $t_\sigma = -t$ and $c_1 = 0$. The (red) thick line is the narrow WSM phase induced by Ir correlation. The dashed line is the nonmagnetic Ir semimetal phase. The green region is the broad WSM phase after including $f$-$d$ exchange. All-in all-out magnetic order is present throughout the phase diagram.

$Nd_2Ir_2O_7$ has been observed to order magnetically below the metal-insulator transition at $T_c = 36$ K.[23–25,31] Recent neutron scattering experiments[25] on $Nd_2Ir_2O_7$ suggest an all-in all-out spin configuration for both Nd and Ir systems. The data were interpreted in terms of a static local field setting in for the Nd moments immediately upon cooling through $T_c$, while Nd magnetic order is not detected until 15 K. Another experiment[24] finds that applying pressure to $Nd_2Ir_2O_7$ suppresses the metal-insulator transition and leads to a metallic state that exhibits a negative magnetoresistance. Since $\Theta_{CW} = -19$ K in $Nd_2Ir_2O_7$, according to Figs. 2(c) and 2(d) we expect $Nd_2Ir_2O_7$ to be in the region with $\Phi < 0$ in order to have an antiferromagnetic $\Theta_{CW}$. Moreover, $T_c > |\Theta_{CW}|$ and the all-in all-out ordering are also consistent with Figs. 2(c) and 2(d). The metal-insulator transition and magnetic order are likely driven by a combination of RKKY exchange and Ir magnetic exchange. Indeed, Ref. 25 interpreted their results in terms of Ir magnetic order setting in at $T_c$, with Nd order setting in only at 15 K (driven by $f$-$d$ exchange) due to the presumably small Ir ordered moment. It would be interesting to see whether our model can indeed produce such behavior at finite temperature. Assuming all-in all-out ordering is indeed present, the Ir electrons may realize a WSM phase within the magnetically ordered state. Indeed, the transport properties of the WSM are close to those of an insulator,[41] and appear consistent with the resistivity of the Nd compound below $T_c$. Applying pressure to $Nd_2Ir_2O_7$[24] may modify the Ir electron hopping, generating a metallic state.

To summarize, we have constructed and analyzed a minimal model accounting for $f$-$d$ exchange in rare-earth-based pyrochlore iridates $R_2Ir_2O_7$. With this model we find broad regions of Axion insulator and Weyl semimetal phases.

We are grateful for helpful discussion with L. Balents, A. Essin, Y.-B. Kim, S. Onoda, Y. Ran, Fa Wang, and W. Witczak-Krempa, and useful correspondence with X. Wan. This work is supported by DOE Award No. DE-SC0003910. Some of this work was carried out at the Aspen Center for Physics and the Kavli Institute for Theoretical Physics; our stays there were supported in part by NSF Grants No. 1066293 and No. PHY11-25915, respectively.

## APPENDIX A: $f$-$d$ EXCHANGE BETWEEN THE R MOMENT AND IR MOMENT

Both Ir and R sublattices are pyrochlore lattices, and can be viewed as fcc lattices with a four-site basis. We use the BCC primitive vectors

$$\mathbf{b}_1 = \left(0,\tfrac{1}{2},\tfrac{1}{2}\right), \tag{A1}$$

$$\mathbf{b}_2 = \left(\tfrac{1}{2},0,\tfrac{1}{2}\right), \tag{A2}$$

$$\mathbf{b}_3 = \left(\tfrac{1}{2},\tfrac{1}{2},0\right). \tag{A3}$$

For the Ir pyrochlore lattice we choose the following reference points for four sublattices:

$$\mathrm{Ir}_1 = \tfrac{1}{4}(0,0,0), \tag{A4}$$

$$\mathrm{Ir}_2 = \tfrac{1}{4}(0,1,1), \tag{A5}$$

$$\mathrm{Ir}_3 = \tfrac{1}{4}(1,0,1), \tag{A6}$$

$$\mathrm{Ir}_4 = \tfrac{1}{4}(1,1,0). \tag{A7}$$

For the R pyrochlore lattice, we choose

$$\mathrm{R}_1 = \left(0,\tfrac{1}{2},0\right), \tag{A8}$$

$$\mathrm{R}_2 = \left(0,\tfrac{3}{4},\tfrac{1}{4}\right), \tag{A9}$$

$$\mathrm{R}_3 = \left(\tfrac{1}{4},\tfrac{1}{2},\tfrac{1}{4}\right), \tag{A10}$$

$$\mathrm{R}_4 = \left(\tfrac{1}{4},\tfrac{3}{4},0\right). \tag{A11}$$

The symmetry-allowed $f$-$d$ exchange between the R moment and the Ir moment can be written as

$$\begin{aligned}
\mathcal{H}_{\mathrm{fd}} = \sum_{\mathbf{r}} \tau_1^z(\mathbf{r})\big\{ & c_1\big[j_2^x(\mathbf{r}) + j_2^x(\mathbf{r}-\mathbf{b}_2+\mathbf{b}_3) + j_3^y(\mathbf{r}-\mathbf{b}_2+\mathbf{b}_3) + j_3^y(\mathbf{r}+\mathbf{b}_1-\mathbf{b}_2) + j_4^z(\mathbf{r}) + j_4^z(\mathbf{r}+\mathbf{b}_1-\mathbf{b}_2)\big] \\
& + c_2\big[j_2^y(\mathbf{r}) + j_2^y(\mathbf{r}-\mathbf{b}_2+\mathbf{b}_3) + j_2^z(\mathbf{r}) + j_2^z(\mathbf{r}-\mathbf{b}_2+\mathbf{b}_3) + j_3^x(\mathbf{r}-\mathbf{b}_2+\mathbf{b}_3) + j_3^x(\mathbf{r}+\mathbf{b}_1-\mathbf{b}_2) + j_3^z(\mathbf{r}-\mathbf{b}_2+\mathbf{b}_3) \\
& + j_3^z(\mathbf{r}+\mathbf{b}_1-\mathbf{b}_2) + j_4^x(\mathbf{r}) + j_4^x(\mathbf{r}+\mathbf{b}_1-\mathbf{b}_2) + j_4^y(\mathbf{r}) + j_4^y(\mathbf{r}+\mathbf{b}_1-\mathbf{b}_2)\big]\big\} \\
& + \tau_2^z(\mathbf{r})\big\{c_1\big[j_1^x(\mathbf{r}+\mathbf{b}_1) + j_1^x(\mathbf{r}+\mathbf{b}_1-\mathbf{b}_2+\mathbf{b}_3) - j_4^y(\mathbf{r}+\mathbf{b}_1) - j_4^y(\mathbf{r}+\mathbf{b}_1-\mathbf{b}_2) - j_3^z(\mathbf{r}+\mathbf{b}_1-\mathbf{b}_2) \\
& - j_3^z(\mathbf{r}+\mathbf{b}_1-\mathbf{b}_2+\mathbf{b}_3)\big] + c_2\big[-j_1^y(\mathbf{r}+\mathbf{b}_1) - j_1^y(\mathbf{r}+\mathbf{b}_1-\mathbf{b}_2+\mathbf{b}_3) - j_1^z(\mathbf{r}+\mathbf{b}_1) - j_1^z(\mathbf{r}+\mathbf{b}_1-\mathbf{b}_2+\mathbf{b}_3) \\
& + j_4^x(\mathbf{r}+\mathbf{b}_1-\mathbf{b}_2) + j_4^x(\mathbf{r}+\mathbf{b}_1) - j_4^z(\mathbf{r}+\mathbf{b}_1-\mathbf{b}_2) - j_4^z(\mathbf{r}+\mathbf{b}_1) + j_3^x(\mathbf{r}+\mathbf{b}_1-\mathbf{b}_2) + j_3^x(\mathbf{r}+\mathbf{b}_1-\mathbf{b}_2+\mathbf{b}_3) \\
& - j_3^y(\mathbf{r}+\mathbf{b}_1-\mathbf{b}_2) - j_3^y(\mathbf{r}+\mathbf{b}_1-\mathbf{b}_2+\mathbf{b}_3)\big]\big\} + \tau_3^z(\mathbf{r})\big\{c_1\big[j_1^y(\mathbf{r}+\mathbf{b}_3) + j_1^y(\mathbf{r}+\mathbf{b}_1) - j_2^z(\mathbf{r}) - j_2^z(\mathbf{r}+\mathbf{b}_3) \\
& - j_4^x(\mathbf{r}) - j_4^x(\mathbf{r}+\mathbf{b}_1)\big] + c_2\big[-j_1^x(\mathbf{r}+\mathbf{b}_3) - j_1^x(\mathbf{r}+\mathbf{b}_1) - j_1^z(\mathbf{r}+\mathbf{b}_3) - j_1^z(\mathbf{r}+\mathbf{b}_1) - j_2^x(\mathbf{r}) - j_2^x(\mathbf{r}+\mathbf{b}_3) \\
& + j_2^y(\mathbf{r}) + j_2^y(\mathbf{b}_3) + j_4^y(\mathbf{r}) + j_4^y(\mathbf{r}+\mathbf{b}_1) - j_4^z(\mathbf{r}) - j_4^z(\mathbf{r}+\mathbf{b}_1)\big]\big\} + \tau_4^z(\mathbf{r})\big\{c_1\big[j_1^z(\mathbf{r}+\mathbf{b}_3) + j_1^z(\mathbf{r}+\mathbf{b}_1-\mathbf{b}_2+\mathbf{b}_3) \\
& - j_2^y(\mathbf{r}-\mathbf{b}_2+\mathbf{b}_3) - j_2^y(\mathbf{r}-\mathbf{b}_2+\mathbf{b}_3) - j_3^x(\mathbf{r}-\mathbf{b}_2+\mathbf{b}_3) - j_3^x(\mathbf{r}+\mathbf{b}_1-\mathbf{b}_2+\mathbf{b}_3)\big] + c_2\big[-j_1^x(\mathbf{r}+\mathbf{b}_3) \\
& - j_1^x(\mathbf{r}+\mathbf{b}_1-\mathbf{b}_2+\mathbf{b}_3) - j_1^y(\mathbf{r}+\mathbf{b}_3) - j_1^y(\mathbf{r}+\mathbf{b}_1-\mathbf{b}_2+\mathbf{b}_3) - j_2^x(\mathbf{r}-\mathbf{b}_2+\mathbf{b}_3) - j_2^x(\mathbf{r}+\mathbf{b}_3) + j_2^z(\mathbf{r}-\mathbf{b}_2+\mathbf{b}_3) \\
& + j_2^z(\mathbf{r}+\mathbf{b}_3) - j_3^y(\mathbf{r}-\mathbf{b}_2+\mathbf{b}_3) - j_3^y(\mathbf{r}+\mathbf{b}_1-\mathbf{b}_2+\mathbf{b}_3) + j_3^z(\mathbf{r}-\mathbf{b}_2+\mathbf{b}_3) + j_3^z(\mathbf{r}+\mathbf{b}_1-\mathbf{b}_2+\mathbf{b}_3)\big]\big\}. \qquad \text{(A12)}
\end{aligned}$$

Here $\tau_i^z(\mathbf{r})$ is the pseudospin for the R site in unit cell labeled by $\mathbf{r}$ with sublattice index $i = 1,\ldots,4$. (Recall that $\tau^z$ is the component of pseudospin along the local threefold axis at the R site.) Similarly, $j_i^\mu(\mathbf{r})$ is the $\mu = x,y,z$ component of the Ir

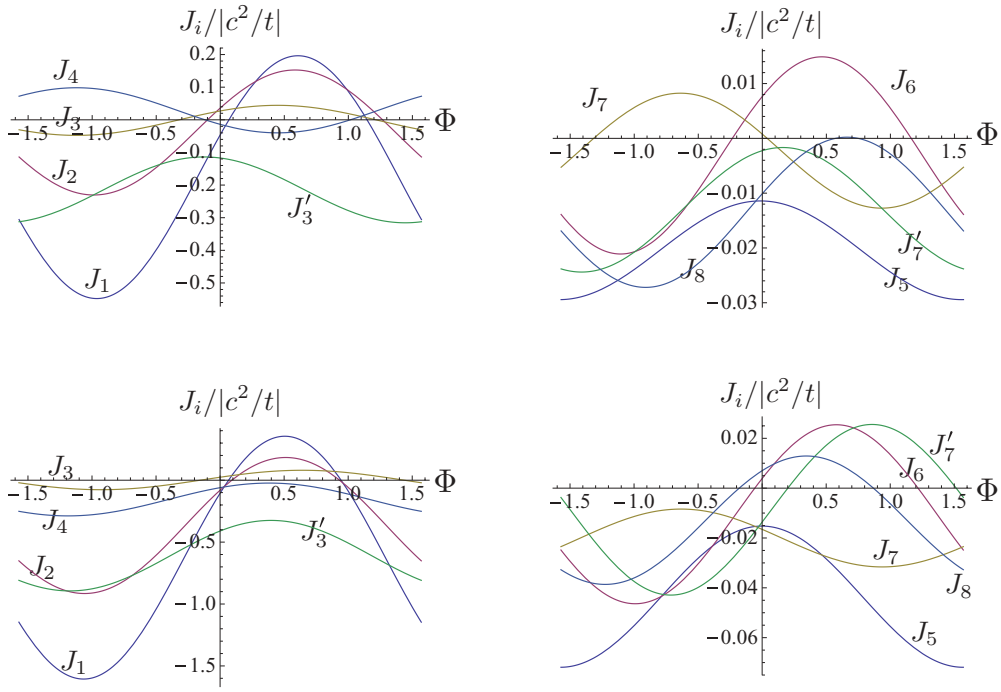


FIG. 5. (Color online) The dependence of RKKY exchanges on the angle $\Phi$. The results are obtained for a finite system with $10 \times 10 \times 10$ unit cells. $J_i$ is the $i$th neighbor exchange. $J_3$ is the exchange on third neighbor bonds that have one lattice site at the midpoint of the bonds. $J_3'$ is the exchange on third neighbor bonds that have no lattice site at the midpoint of the bonds. $J_7$ is the exchange on seventh neighbor bonds that have two additional lattice sites along the bonds. $J_7'$ is the exchange on seventh neighbor bonds that have no lattice sites along the bonds. Upper: STI phase with $t_\sigma = -2t$. Lower: Semimetal phase with $t_\sigma = -t$.

effective spin (in global cubic coordinates), for the Ir site in unit cell $\mathbf{r}$ at sublattice $i$. $c_1$ and $c_2$ are the two parameters allowed by space group symmetries.

It is convenient below to work in a local coordinate system for the Ir effective moment. So, we transform the Ir effective spin from glocal to local $IrO_6$ octahedral coordinate system by

$$j_i^\mu(\mathbf{r}) = \mathcal{R}_i^{\mu\nu} j_{i,L}^\nu(\mathbf{r}), \tag{A13}$$

where $\mathbf{j}_{i,L}(\mathbf{r})$ is the Ir effective spin in the local $IrO_6$ octahedral coordinate system. The transformation matrices for four sublattices are

$$\mathcal{R}_1 = \begin{bmatrix} 2/3 & -1/3 & -2/3 \\ -1/3 & 2/3 & -2/3 \\ 2/3 & 2/3 & 1/3 \end{bmatrix}, \tag{A14}$$

$$\mathcal{R}_2 = \begin{bmatrix} 2/3 & 2/3 & 1/3 \\ -2/3 & 1/3 & 2/3 \\ 1/3 & -2/3 & 2/3 \end{bmatrix}, \tag{A15}$$

$$\mathcal{R}_3 = \begin{bmatrix} 1/3 & -2/3 & 2/3 \\ 2/3 & 2/3 & 1/3 \\ -2/3 & 1/3 & 2/3 \end{bmatrix}, \tag{A16}$$

$$\mathcal{R}_4 = \begin{bmatrix} 1/3 & -2/3 & 2/3 \\ -2/3 & -2/3 & -1/3 \\ 2/3 & -1/3 & -2/3 \end{bmatrix}. \tag{A17}$$

## APPENDIX B: RKKY INTERACTION BETWEEN THE R MOMENTS

We consider the Hamiltonian

$$\mathcal{H} = \mathcal{H}_{\rm Ir} + \mathcal{H}_{\rm fd}, \tag{B1}$$

where $\mathcal{H}_{\rm Ir}$ is the tight-binding Hamiltonian without the Hubbard interaction,

$$\mathcal{H}_{\rm Ir} = \sum_{\langle rr'\rangle} \left(\mathcal{T}^d_{rr',\alpha\beta} + \mathcal{T}^{\rm id}_{rr',\alpha\beta}\right) d^\dagger_{r\alpha} d_{r'\beta}. \tag{B2}$$

The $f$-$d$ exchange $\mathcal{H}_{\rm fd}$ can be written compactly as

$$\mathcal{H}_{\rm fd} = \sum_{\mathbf{r},\mathbf{r}'} \sum_{ij} \tau_i^z(\mathbf{r}) f_{ij}^\mu(\mathbf{r}-\mathbf{r}') j_j^\mu(\mathbf{r}'). \tag{B3}$$

Here, and below, sums on repeated indices are implied. The exchange is characterized by the function $f_{ij}^\mu(\mathbf{r})$, which can be read off from Eq. (A12).

Diagonalizing the tight-binding Hamiltonian $\mathcal{H}_{\rm Ir}$ gives

$$\mathcal{H}_{\rm Ir} = \sum_{\mathbf{k},\lambda} \epsilon_{\mathbf{k}\lambda} c^\dagger_{\mathbf{k}\lambda} c_{\mathbf{k}\lambda}, \tag{B4}$$

where $\lambda$ labels the eight eigenstates for each $\mathbf{k}$, and

$$d^\dagger_{\mathbf{k}i\alpha} = \sum_\lambda c^\dagger_{\mathbf{k}\lambda} \mathcal{U}_{\lambda,i\alpha}(\mathbf{k}). \tag{B5}$$

We now treat $\mathcal{H}_{\rm fd}$ as a perturbation to the Ir tight-binding Hamiltonian $\mathcal{H}_{\rm Ir}$. By standard second-order perturbation

theory, we obtain the effective RKKY exchange between the local moments of the R subsystem,

$$\mathcal{H}_{\mathrm{RKKY}} = \sum_i \frac{\langle\Phi_0|\mathcal{H}_{\mathrm{fd}}|\Phi_i\rangle\langle\Phi_i|\mathcal{H}_{\mathrm{fd}}|\Phi_0\rangle}{E_0 - E_i}, \tag{B6}$$

in which $|\Phi_0\rangle$ and $E_0$ are the ground state and the corresponding energy, and $|\Phi_i\rangle$ and $E_i$ are the $i$th excited state and the corresponding energy. This result can be written

$$\mathcal{H}_{\mathrm{RKKY}} = \frac{1}{2}\sum_{\mathbf{r}_1 i_1,\mathbf{r}_2 i_2} J_{i_1 i_2}(\mathbf{r}_1 - \mathbf{r}_2)\tau^z_{i_1}(\mathbf{r}_1)\tau^z_{i_2}(\mathbf{r}_2), \tag{B7}$$

with $J_{i_1 i_2}(\mathbf{r}_1 - \mathbf{r}_2) \equiv \tilde{J}_{i_1 i_2}(\mathbf{r}_1 - \mathbf{r}_2) + \tilde{J}_{i_2 i_1}(\mathbf{r}_2 - \mathbf{r}_1)$, where

$$\begin{aligned}\tilde{J}_{i_1 i_2}(\mathbf{r}_1 - \mathbf{r}_2) = \frac{1}{4}\sum_{\mathbf{r}'_1,\mathbf{r}'_2} & f^{\mu_1}_{i_1 j_1}(\mathbf{r}_1 - \mathbf{r}'_1) f^{\mu_2}_{i_2 j_2}(\mathbf{r}_2 - \mathbf{r}'_2)\mathcal{R}^{\mu_1\nu_1}_{j_1}\mathcal{R}^{\mu_2\nu_2}_{j_2} \\ & \times \sigma^{\nu_1}_{\alpha_1\beta_1}\sigma^{\nu_2}_{\alpha_2\beta_2}\frac{1}{N_c^2}\sum_{\mathbf{k}_1,\mathbf{k}_2} e^{i(\mathbf{k}_2-\mathbf{k}_1)\cdot(\mathbf{r}'_1-\mathbf{r}'_2)}\mathcal{U}_{\lambda_1, j_1\alpha_1} \\ & \times (\mathbf{k}_1)\mathcal{U}^*_{\lambda_1, j_2\beta_2}(\mathbf{k}_1)\mathcal{U}_{\lambda_2, j_2\alpha_2}(\mathbf{k}_2)\mathcal{U}^*_{\lambda_2, j_1\beta_1}(\mathbf{k}_2) \\ & \times \frac{\Theta\left[\epsilon_F - \epsilon_{\lambda_1}(\mathbf{k}_1)\right]\Theta\left[\epsilon_{\lambda_2}(\mathbf{k}_2) - \epsilon_F\right]}{\epsilon_{\lambda_1}(\mathbf{k}_1) - \epsilon_{\lambda_2}(\mathbf{k}_2)}.\end{aligned} \tag{B8}$$

Here $\sigma^\nu$ is the Pauli matrix, $N_c$ is the number of unit cell, and $\Theta(x)$ is the Heaviside step function.

Since the RKKY exchanges are quadratic in $c_1$ and $c_2$, we can simply focus on the regime with $c_1 \geqslant 0$ and define an angle $\Phi \equiv \tan^{-1}(c_2/c_1)$ and $c \equiv \sqrt{c_1^2 + c_2^2}$. As shown in Fig. 5, we compute the RKKY exchanges of a finite system with $10 \times 10 \times 10$ unit cells for both the STI phase with $t_\sigma = -2t$ and the semimetal phase with $t_\sigma = -t$. Clearly the RKKY exchanges beyond fourth neighbor become significantly smaller. We now focus on the truncated RKKY exchanges up to fourth neighbor. The Curie-Weiss temperature is found to be

$$\Theta_{\mathrm{CW}} = \tfrac{1}{2}(J_1 + 2J_2 - 3J_3 - 3J'_3 + 2J_4). \tag{B9}$$

The transition from the high-temperature paramagnetic phase to low-temperature ordered phase is continuous at mean-field level. The transition from paramagnetic phase to all-in all-out state is of three-dimensional Ising type. We can then determine the critical temperatures for this transition by the usual condition of marginal stability (vanishing of the quadratic term in the Landau theory) of the free energy. Restricting to $\mathbf{q} = \mathbf{0}$ magnetic order, we find that the critical temperatures for all-in all-out and two-in two-out states are given by

$$T_c(\text{all-in all-out}) = \tfrac{1}{2}(-J_1 - 2J_2 - J_3 - J'_3 - 2J_4), \tag{B10}$$

$$T_c(\text{two-in two-out}) = \tfrac{1}{6}(J_1 + 2J_2 - 3J_3 - 3J'_3 + 2J_4), \tag{B11}$$

respectively. The actual transition temperature is determined by the higher one of the above transition temperatures.


[1] M. Z. Hasan and C. L. Kane, Rev. Mod. Phys. **82**, 3045 (2010).
[2] X.-L. Qi and S.-C. Zhang, Rev. Mod. Phys. **83**, 1057 (2011).
[3] M. Z. Hasan and J. E. Moore, Annu. Rev. Cond. Matt. Phys. **2**, 55 (2011).
[4] D. Pesin and L. Balents, Nat. Phys. **6**, 376 (2010).
[5] X. Wan, A. M. Turner, A. Vishwanath, and S. Y. Savrasov, Phys. Rev. B **83**, 205101 (2011).
[6] W. Witczak-Krempa and Y. B. Kim, Phys. Rev. B **85**, 045124 (2012).
[7] A. Go, W. Witczak-Krempa, G. S. Jeon, K. Park, and Y. B. Kim, Phys. Rev. Lett. **109**, 066401 (2012).
[8] X.-L. Qi, T. L. Hughes, and S.-C. Zhang, Phys. Rev. B **78**, 195424 (2008).
[9] A. M. Essin, J. E. Moore, and D. Vanderbilt, Phys. Rev. Lett. **102**, 146805 (2009).
[10] T. L. Hughes, E. Prodan, and B. A. Bernevig, Phys. Rev. B **83**, 245132 (2011).
[11] A. M. Turner, Y. Zhang, R. S. K. Mong, and A. Vishwanath, Phys. Rev. B **85**, 165120 (2012).
[12] X. Wan, A. Vishwanath, and S. Y. Savrasov, Phys. Rev. Lett. **108**, 146601 (2012).
[13] W. Witczak-Krempa, A. Go, and Y. B. Kim, arXiv:1208.4099.
[14] J. S. Gardner, M. J. P. Gingras, and J. E. Greedan, Rev. Mod. Phys. **82**, 53 (2010).
[15] S. Onoda and Y. Tanaka, Phys. Rev. Lett. **105**, 047201 (2010).
[16] S. Onoda and Y. Tanaka, Phys. Rev. B **83**, 094411 (2011).
[17] L. Savary and L. Balents, Phys. Rev. Lett. **108**, 037202 (2012).
[18] S. Lee, S. Onoda, and L. Balents, arXiv:1204.2262.
[19] L. D. C. Jaubert, S. Piatecki, M. Haque, and R. Moessner, Phys. Rev. B **85**, 054425 (2012).
[20] M. Udagawa, H. Ishizuka, and Y. Motome, Phys. Rev. Lett. **108**, 066406 (2012).
[21] H. Ishizuka, M. Udagawa, and Y. Motome, J. Phys. Soc. Jpn. **81**, 113706 (2012).
[22] Y. Machida, S. Nakatsuji, S. Onoda, T. Tayama, and T. Sakakibara, Nature (London) **463**, 210 (2010).
[23] K. Matsuhira, M. Wakeshima, R. Nakanishi, T. Yamada, A. Nakamura, W. Kawano, S. Takagi, and Y. Hinatsu, J. Phys. Soc. Jpn. **76**, 043706 (2007).
[24] M. Sakata, T. Kagayama, K. Shimizu, K. Matsuhira, S. Takagi, M. Wakeshima, and Y. Hinatsu, Phys. Rev. B **83**, 041102 (2011).
[25] K. Tomiyasu, K. Matsuhira, K. Iwasa, M. Watahiki, S. Takagi, M. Wakeshima, Y. Hinatsu, M. Yokoyama, K. Ohoyama, and K. Yamada, J. Phys. Soc. Jpn. **81**, 034709 (2012).
[26] D. Yanagishima and Y. Maeno, J. Phys. Soc. Jpn. **70**, 2880 (2001).
[27] S. M. Disseler, C. Dhital, T. C. Hogan, A. Amato, S. R. Giblin, C. de la Cruz, A. Daoud-Aladine, S. D. Wilson, and M. J. Graf, Phys. Rev. B **85**, 174441 (2012).
[28] B. D. Gaulin, J. S. Gardner, P. A. McClarty, and M. J. P. Gingras, Phys. Rev. B **84**, 140402 (2011).
[29] M. J. Harris, S. T. Bramwell, D. F. McMorrow, T. Zeiske, and K. W. Godfrey, Phys. Rev. Lett. **79**, 2554 (1997).
[30] Y. Machida, Ph.D. thesis, Kyoto University, Japan, 2006.
[31] M. Watahiki, K. Tomiyasu, K. Matsuhira, K. Iwasa, M. Yokoyama, S. Takagi, M. Wakeshima, and Y. Hinatsu, J. Phys.: Conf. Ser. **320**, 012080 (2011).

[32]K. Matsuhira, Y. Hinatsu, K. Tenya, H. Amitsuka, and T. Sakakibara, J. Phys. Soc. Jpn. **71**, 1576 (2002).
[33]S. Nakatsuji *et al.*, Phys. Rev. Lett. **96**, 087204 (2006).
[34]J. E. Moore and L. Balents, Phys. Rev. B **75**, 121306 (2007).
[35]L. Fu, C. L. Kane, and E. J. Mele, Phys. Rev. Lett. **98**, 106803 (2007).
[36]R. Roy, Phys. Rev. B **79**, 195322 (2009).
[37]X. Wan (private communication).
[38]J. M. Luttinger and L. Tisza, Phys. Rev. **70**, 954 (1946).
[39]We add a small second neighbor hopping ($t'_\sigma = 0.04t_\sigma$ and $t'_\pi = 0.04t_\pi$) to break the flatness along the $\Gamma$-$L$ lines.
[40]Y. Machida, S. Nakatsuji, Y. Maeno, T. Tayama, T. Sakakibara, and S. Onoda, Phys. Rev. Lett. **98**, 057203 (2007).
[41]P. Hosur, S. A. Parameswaran, and A. Vishwanath, Phys. Rev. Lett. **108**, 046602 (2012).